Experimental Animals
Exp. Anim. 71(1), 14–21, 2022

Original

Mitochondrial DNA deletion-dependent podocyte injuries in Mito-miceΔ, a murine model of mitochondrial disease

Shuzo KANEKO[1], Joichi USUI[1], Masahiro HAGIWARA[1]*, Tatsuya SHIMIZU[1], Ryota ISHII[1], Mayumi TAKAHASHI-KOBAYASHI[1], Mikiko KAGEYAMA[1], Kazuto NAKADA[2], Jun-Ichi HAYASHI[3] and Kunihiro YAMAGATA[1]

[1]*Department of Nephrology, Faculty of Medicine, University of Tsukuba, 1-1-1 Tennodai, Tsukuba, Ibaraki 3058575, Japan*
[2]*Fuculty of Life and Environmental Sciences, University of Tsukuba, 1-1-1 Tennodai, Tsukuba, Ibaraki 3058572, Japan*
[3]*Life Science Center for Survival Dynamics, Tsukuba Advanced Research Alliance (TARA), University of Tsukuba, 1-1-1 Tennodai, Tsukuba, Ibaraki 3058572, Japan*
**Present address: Saku Central Hospital, 197 Usuda, Saku, Nagano 3840301, Japan*

Abstract: Focal segmental glomerulosclerosis (FSGS) is a major renal complication of human mitochondrial disease. However, its pathogenesis has not been fully explained. In this study, we focused on the glomerular injury of mito-miceΔ and investigated the pathogenesis of their renal involvement. We analyzed biochemical data and histology in mito-miceΔ. The proteinuria began to show in some mito-miceΔ with around 80% of mitochondrial DNA deletion, then proteinuria developed dependent with higher mitochondrial DNA deletion, more than 90% deletion. Mito-miceΔ with proteinuria histologically revealed FSGS. Immunohistochemistry demonstrated extensive distal tubular casts due to abundant glomerular proteinuria. Additionally, the loss of podocyte-related protein and podocyte's number were found. Therefore, the podocyte injuries and its depletion had a temporal relationship with the development of proteinuria. This study suggested mitochondrial DNA deletion-dependent podocyte injuries as the pathogenesis of renal involvement in mito-miceΔ. The podocytes are the main target of mitochondrial dysfunction originated from the accumulation of mitochondrial DNA abnormality in the kidney.
Key words: focal segmental glomerulosclerosis, mitochondrial disease model, mitochondrial DNA deletion, podocyte injury

Introduction

Mitochondrial disease can affect various organs including the kidneys [1–3]. Several studies have reported that patients with the m.3243A>G mutation develop focal segmental glomerulosclerosis (FSGS) as renal involvement [4]. Among these cases, electron microscopy demonstrated abnormal mitochondria in podocytes, not only in tubular epithelial cells [5, 6]. The previous case report suggested the relationship between podocyte injury and FSGS in mitochondrial disease [7]. However, there is as yet no convincing evidence to explain podocyte injury is the direct outcome of mitochondrial dysfunction.

Mito-miceΔ are mouse models for mitochondrial disease with a heteroplasmic state for wild-type mitochondrial DNA (mtDNA) and pathogenic mtDNA having a large-scale deletion (ΔmtDNA) [8]. Mito-miceΔ develop clinical phenotypes (retinal abnormality, anemia, movement disorder, myopathy, deafness, cardiac conduction disorder and male infertility), only if the proportion of ΔmtDNA in each organ reaches higher than 70–80% [9–13]. This phenomenon is called threshold effect and is also well-described in human cases [14]. Renal in-

(Received 23 March 2021 / Accepted 5 July 2021 / Published online in J-STAGE 28 July 2021)
Corresponding author: K. Yamagata. email: k-yamaga@md.tsukuba.ac.jp

volvement is a major feature of mito-miceΔ. In the previous studies, mito-miceΔ with the renal proportion of ΔmtDNA exceeding 85% showed deterioration of cytochrome c oxidase (COX) activity and histological change including FSGS and tubular dilatation with casts [8, 9].

Mito-miceΔ manifest renal involvement resembling that of human mitochondrial disease. Although it has been suggested that mitochondrial respiratory defect is essential for the pathogenesis, the specific role of each cell in the kidneys remains unclear [9]. In the present study, we focused on the podocyte injury of mito-miceΔ.

Materials and Methods

Mice

Mito-miceΔ were generated by introduction of ΔmtDNA from cultivated cells into fertilized eggs of F1 female mice (B6D2F1, obtained by crossing C57BL/6J and DBA/2) using cell fusion techniques as described previously [8]. We used 12 to 25 week-old non-castrated male mito-miceΔ carrying various proportions of ΔmtDNA (n=18) and wild-type male C57BL/6J mice (n=3) as a control for the study. Animal experiments were performed in accordance with protocols approved by the Experimental Animal Committee of the University of Tsukuba.

Estimation of ΔmtDNA proportions

Total DNA were extracted by DNeasy Tissue Kit® (QIAGEN sciences, MD) according to manufacture recommendation. Total RNA was extracted from renal cortex by SV total RNA isolation system® (Promega, Madison, WI, USA) according to manufacture recommendation. The proportion of wild-type mtDNA and ΔmtDNA was calculated by real-time PCR analysis as described previously [8]. First, we measured the proportion of ΔmtDNA in tail samples from all 4 week-old mice because they represent the proportions of ΔmtDNA in different organs from the same individual [9]. Subsequently, we sacrificed 12 to 25 week-old mice for examination and calculated the renal proportions of ΔmtDNA.

The measurement of urinary protein, BUN and serum creatinine

Spot urine samples were collected. Urinary protein was measured by Bio-Rad Protein Assay (Bio-Rad Laboratories, CA), determined by Bradford method. Urinary creatinine was measured using Dimension ARX 990390-X (Siemens Healthcare Diagnostics, Tokyo, Japan). Urinary protein value was expressed as g/gCr. BUN and serum creatinine were measured using a Dry-Chem 3500 automated analyzer (Fuji Film Inc., Tokyo, Japan).

Histological analysis

Kidneys were fixed with 10% formaldehyde and embedded in paraffin or fixed with 4% paraformaldehyde for frozen sections, in Optimal Cutting Temperature compound (Sakura Finetek, Tokyo, Japan). Paraffin sections were deparaffinized with xylene and hydrated with graded ethanols. A microwave oven was used for antigen retrieval.

Paraffin sections were stained with hematoxylin and eosin (HE), periodic acid Schiff (PAS), periodic acid-methenamine silver (PAM) or Masson trichrome (MT) for light microscopy. We counted the number of total glomeruli in random one cross section of a kidney in PAM sections of each mouse and estimated the percentage of glomeruli with FSGS. Sclerosing lesion involving more than 50% of affected glomeruli was defined as global sclerosis, and less than 50% as segmental lesion. Severity of tubular dilatation and interstitial fibrosis was evaluated in MT sections.

Paraffin sections were stained immunohistochemically. Briefly, each section was incubated with primary antibody for 2 h at room temperature and with secondary antibody for 30 min at room temperature. Primary antibodies were anti-aquaporin 1 (AQP1) antibody (polyclonal rabbit IgG, 1:400 dilution; Chemicon International, Temecula, CA), anti-Tamm-Horsfall glycoprotein (THP) antibody (goat antiserum, 1:1,000 dilution; MP Biomedicals, Solon, OH, USA), and anti- Wilms tumor 1 (WT1) antibody (polyclonal rabbit IgG, 1:50 dilution, Santa Cruz Biotechnology, Santa Cruz, CA, USA). We used Fab'-conjugated peroxidase-labeled amino acid polymer (Histofine® Simple Stain™ MAX PO; Nichirei Biosciences, Tokyo, Japan) or biotinylated goat anti-rabbit IgG (Vector Laboratories, Burlingame, CA, USA) and streptavidin-conjugated horseradish peroxidase complex incubation as secondary antibody, followed by diaminobenzidine (DAB) staining.

Frozen sections were stained immunohistochemically. As primary antibodies, rabbit polyclonal antibodies recognizing C terminal sequence of both nephrin and podocin (nephrin: CEDPRGIYDQVAADMD (neph-C: 1212–1226), podocin: CVEPLNPKKKDSPML (pod-C: 372–385)) were generated (QIAGEN, Peptide synthesis service, Tokyo, Japan). The antigen specificity of these two antibodies was confirmed by the specific band on western blot using normal kidney of C57BL/6J mice (data not shown). We used Alexa Fluor 488-conjugated anti-rabbit IgG (1:400 dilution, Invitrogen, San Diego, CA, USA) as secondary antibody.

Electron microscopy

For ultrastructural analysis of glomerulus, murine kidneys were cut into tissue blocks (approximately 0.5 mm^3) and immersed in 2.5% phosphate-buffered glutaraldehyde overnight at 4 degrees. The tissue blocks were postfixed in 1% osmium tetroxide for 2 h at 4 degrees, dehydrated in graded ethanols, and embedded in epoxy resin (Poly/Bed 812 Embedding Media, Polysciences, Warrington, PA). Ultra-thin sections cut on a Leica Ultracut S microtome (Leica, Vienna, Austria) were stained with uranyl acetate and lead citrate. Sections were observed by transmission electron microscopy (TEM) at 75kV using a H-7000 instrument (Hitachi, Tokyo, Japan).

Quantification of WT1 positive cells in glomeruli

To recognize podocyte depletion, we used anti-WT1 antibody and counted the number of WT1 positive cells in glomeruli. Eight kidney samples of mito-miceΔ were selected in a random manner. For estimation of podocyte number, we scanned at least 50 glomeruli in a section. Mito-miceΔ were divided into 2 groups depending on the proportion of ΔmtDNA and were performed nonparametric statistical analysis, Mann-Whitney U test.

Results

The effect of ΔmtDNA accumulation in podocytes induced proteinuria

To delineate renal injury in mito-miceΔ biochemically, we measured urinary protein excretion and the renal proportion of ΔmtDNA at sacrifice. The values for proteinuria were standardized by urinary protein to creatinine ratio (Table 1). In all mito-miceΔ, proportions of ΔmtDNA increased linearly by aging from those in the 4-week tail, probably because smaller ΔmtDNA had a replication advantage over wild-type mtDNA [9]. Some mice with the proportion of ΔmtDNA exceeding 80% (sample No. 11 and 13) began to show proteinuria, and all mice with the proportion of ΔmtDNA exceeding 90% (sample No. 15–18) developed proteinuria (Fig. 1). Mice with the proportion of ΔmtDNA less than 80% or less than 18-week-old mice had no proteinuria (Table 1). Serum creatinine (sCr) and blood urea nitrogen (BUN) value were examined in 2 mito-miceΔ (sample No. 16 and 17). At the time of sacrifice, the data of renal function was as follows: sCr 0.8 mg/dl, BUN 40.1 mg/dl in sample No. 16; sCr 0.4 mg/dl, BUN 21.6 mg/dl in sample No. 17, respectively, indicating a mild renal function deterioration in sample No. 16 mouse. Although the study was limited in number describing only 2 cases, some mice presented with renal failure.

Table 1. Biochemical and histological characteristics of mice

Sample number	Age at sacrifice (weeks)	Proportion of ΔmtDNA 4-week tail (%)	Proportion of ΔmtDNA Kidney at sacrifice (%)	Urinary protein (g/gCr)	Number of total glomeruli	Number of global sclerosis (%)	Number of segmental lesion (%)	Tubular dilatation	Interstitial fibrosis (%)
Control									
B6(12)	12		0	3.9	147	0	0	no	<5
B6(18)	18		0	2.9	211	0	0	no	<5
B6(22)	22		0	3.1	181	0	0	no	<5
Mito-miceΔ									
1	16	14.6	40.5	4.6	170	0	0	no	<5
2	16	27.2	45.2	4.9	168	0	0	no	<5
3	12	67.6	71.9	8.1	88	0	0	no	<5
4	12	68.5	75.0	5.3	78	0	0	no	<5
5	22	37.9	76.0	9.8	93	0	0	no	<5
6	18	60.0	79.3	9.5	76	0	0	no	<5
7	12	60.0	79.4	4.1	215	0	0	no	<5
8	22	29.6	79.4	12.2	70	0	0	no	<5
9	12	62.9	79.6	4.1	66	0	0	no	<5
10	13	73.0	80.1	3.6	163	0	0	no	<5
11	16	69.6	83.7	28.1	183	0	0	no	<5
12	22	60.0	83.9	2.5	147	0	0	no	<5
13	17	60.0	84.0	31.1	157	0	0	no	<5
14	16	66.5	86.1	9.0	237	0	0	no	<5
15	24	68.0	90.8	53.3	159	10 (6.3)	7 (4.4)	yes	<5
16	22	71.2	92.2	85.9	94	22 (23.4)	20 (21.3)	yes	<5
17	22	63.3	92.9	31.9	102	0 (0)	1 (1.0)	yes	<5
18	25	67.0	93.0	42.4	177	1 (0.6)	12 (6.8)	yes	<5

Histology of renal involvements

Mito-miceΔ with the proportion of ΔmtDNA less than 90% did not show any histological change compared with control mice (data not shown). In contrast, mito-miceΔ with the proportion of ΔmtDNA exceeding 90% (sample No. 15–18) developed glomerular involvements including both global sclerosis and segmental lesions with epithelial hyperplasia or adhesion (Fig. 2a). However, the frequency of glomerular involvements varied widely, approximately 1 to 44.7% of glomeruli (Table). Tubular dilatation with casts throughout renal cortex to medulla was also observed in these mice, but interstitial fibrosis was scarcely detected (Figs. 2b and c). The appearance of these tubular casts in medullary rays and deep medulla was originated from massive glomerular proteinuria.

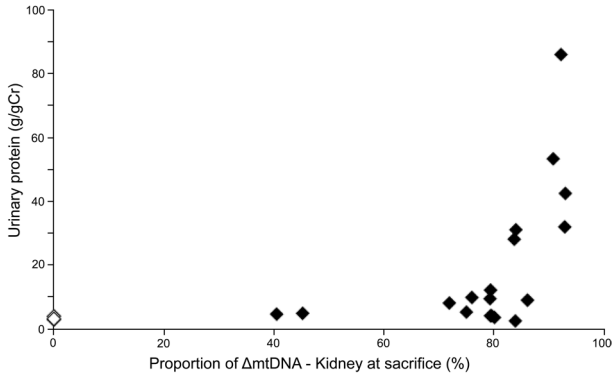

Fig. 1. Effect of ΔmtDNA accumulation on proteinuria. Mito-miceΔ with more than 80% ΔmtDNA in the kidneys developed proteinuria. This is consistent with the previous observations that threshold of mitochondrial respiratory defect in mito-miceΔ was around 85% ΔmtDNA accumulation. ◇B6 control (n=3), ◆mito-miceΔ (n=18).

To clarify the origin of tubular lesions, we performed immunohistochemistry of the tubular markers; AQP1 for proximal tubules and THP for distal tubules. Control mice and mito-miceΔ with less than 90% ΔmtDNA in the kidneys showed the normal expression pattern of these markers. In contrast, dilated tubules of the affected mice (sample No. 15–18) were negative for AQP1 expression (Fig. 3a) and mostly positive for THP (Fig. 3b). These light microscopic and immunohistochemical results showed protein casts in distal tubules originated from massive glomerular proteinuria. Additionally, distal tubular dilation without noticeable interstitial fibrosis suggested that these changes were mainly attributed to the glomerular involvements, not to the tubular involvements. In summary, these histological characters were typical for FSGS, resembling clinical phenotype of nephrotic syndrome in human.

On the electron microscopy, in control mice, mitochondria in podocytes appeared uniform and unnoticeable (data not shown). In contrast, aged mito-miceΔ with

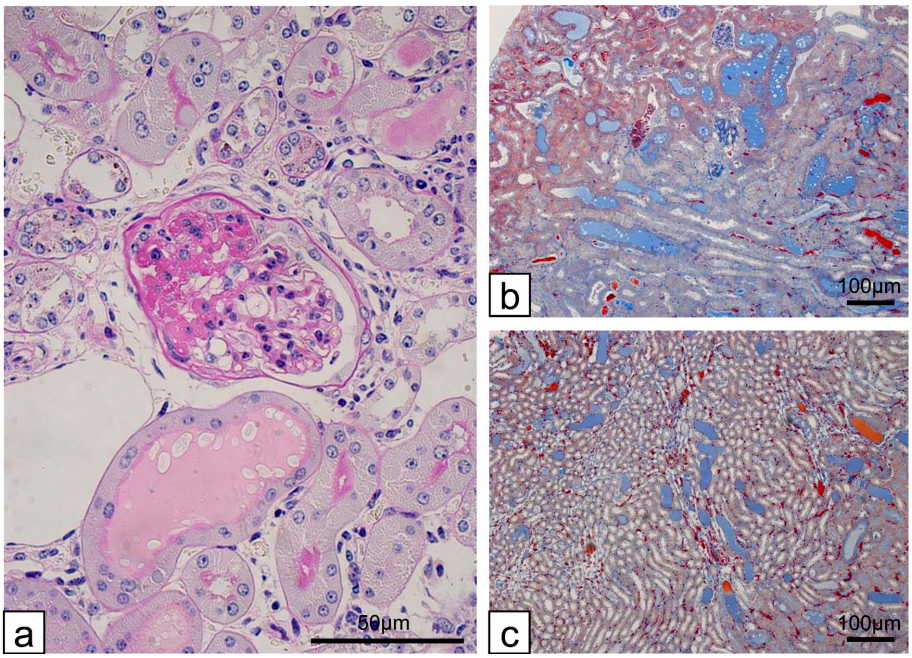

Fig. 2. Light microscopy of glomerular and tubulointerstitial involvements. (a) Sample No. 18 (25 week-old, ΔmtDNA 93.0%). A glomerulus revealed segmental sclerosis on the left side. Some tubular casts were seen. (b), (c) Sample No. 18 (25 week-old, ΔmtDNA 93.0%). Tubular dilatation with hyaline casts was frequently seen in both renal cortex (b) and medulla (c). The appearance of these tubular casts was originated from glomerular proteinuria. (a): PAS stain, (b), (c): MT stain.

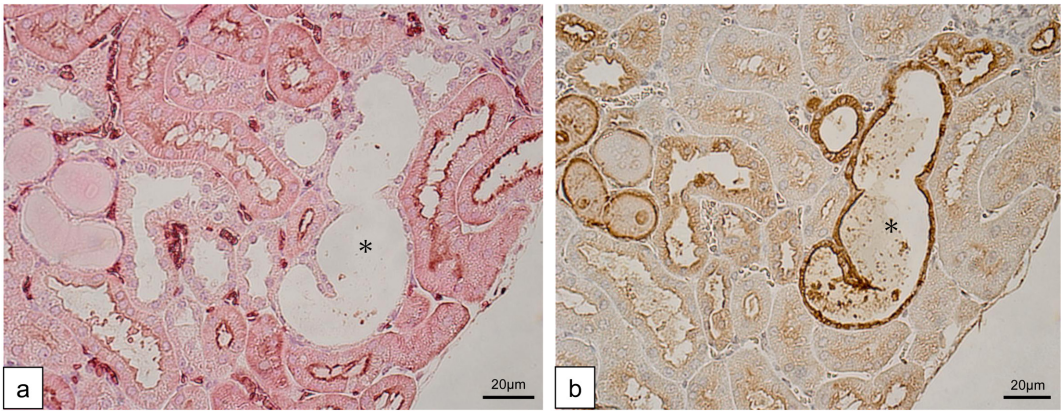

Fig. 3. Immunohistochemistry of tubular involvements. (a) Anti-AQP1 staining in renal cortex. Epithelium of the dilated tubule (black asterisk) was negative for AQP1. (b) Anti-THP staining in renal cortex. Extensive formation of intraluminal THP-positive casts including the AQP1-negative dilated tubule (black asterisk). A large part of the dilated tubules themselves were positive for THP. This implies that the dilated tubules were derived from distal nephrons. Both pictures were continuous sections.

more than 90% ΔmtDNA in the kidneys contained numerous dysmorphic mitochondria in podocytes (Fig. 4). Extensive foot process effacement was also observed in these mice. These electron microscopic findings revealed diffuse podocyte injuries, corresponding to the histology of FSGS.

To detect the change in expression of podocyte protein, immunofluorescence for nephrin and podocin was performed. Control mice showed linear pattern for both proteins along the capillary walls (Figs. 5a and d). As the proportion of ΔmtDNA increased to less than 90%, mito-miceΔ showed almost linear pattern for both proteins (Figs. 5b and e). By contrast, as the proportion of ΔmtDNA increased to more than 90%, mito-miceΔ showed weak and granular pattern for both proteins (Figs. 5c and f). To evaluate podocyte loss in detail, we counted the number of WT1-positive podocytes. In control mice (n=3), the median number of WT1 positive cells per glomerulus was 6.2 cells (Fig. 6a). The number of WT1 positive cells showed a statistically significant decrease in mito-miceΔ with the proportion of ΔmtDNA exceeding a median of 81.7% {Figs. 6a and b, lower proportion of ΔmtDNA group (n=4) with a median of 6.1 cells; higher group (n=4) with a median of 4.5 cells, P=0.029)}.

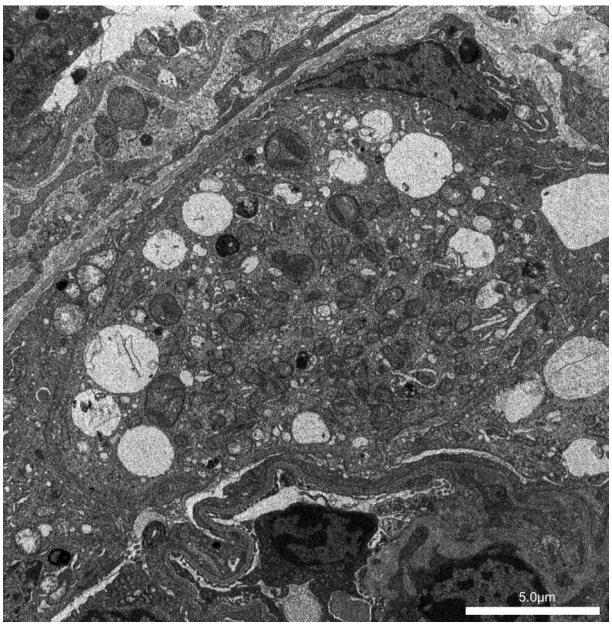

Fig. 4. Electron microscopy for podocyte fine structure. Sample No. 17 (22 week-old, ΔmtDNA 92.9%). Numerous dysmorphic mitochondria were seen in podocyte cytoplasm. Extensive foot process effacement was found.

Discussion

FSGS is a typical glomerular disease based on diffuse podocyte injuries, and recently named as podocytopathy [15–17]. In the present study, we confirmed that mito-miceΔ with over 80% of ΔmtDNA began to appeared proteinuria and podocyte depletion, resulting in FSGS with distal tubular dilatation when ΔmtDNA ratio became higher than 90%. Our results provided a new concept that proteinuria was a biomarker of early stage of kidney involvements in mito-miceΔ and its threshold was around 80% ΔmtDNA accumulation. The threshold of proteinuria corresponded to that of mitochondrial respiratory defect reported in the previous studies [9, 18].

In this study, we investigated the morphologic change, molecular expression and loss of podocyte in mito-miceΔ, focused on both glomerular and tubular involvements. First, we could observe histological findings

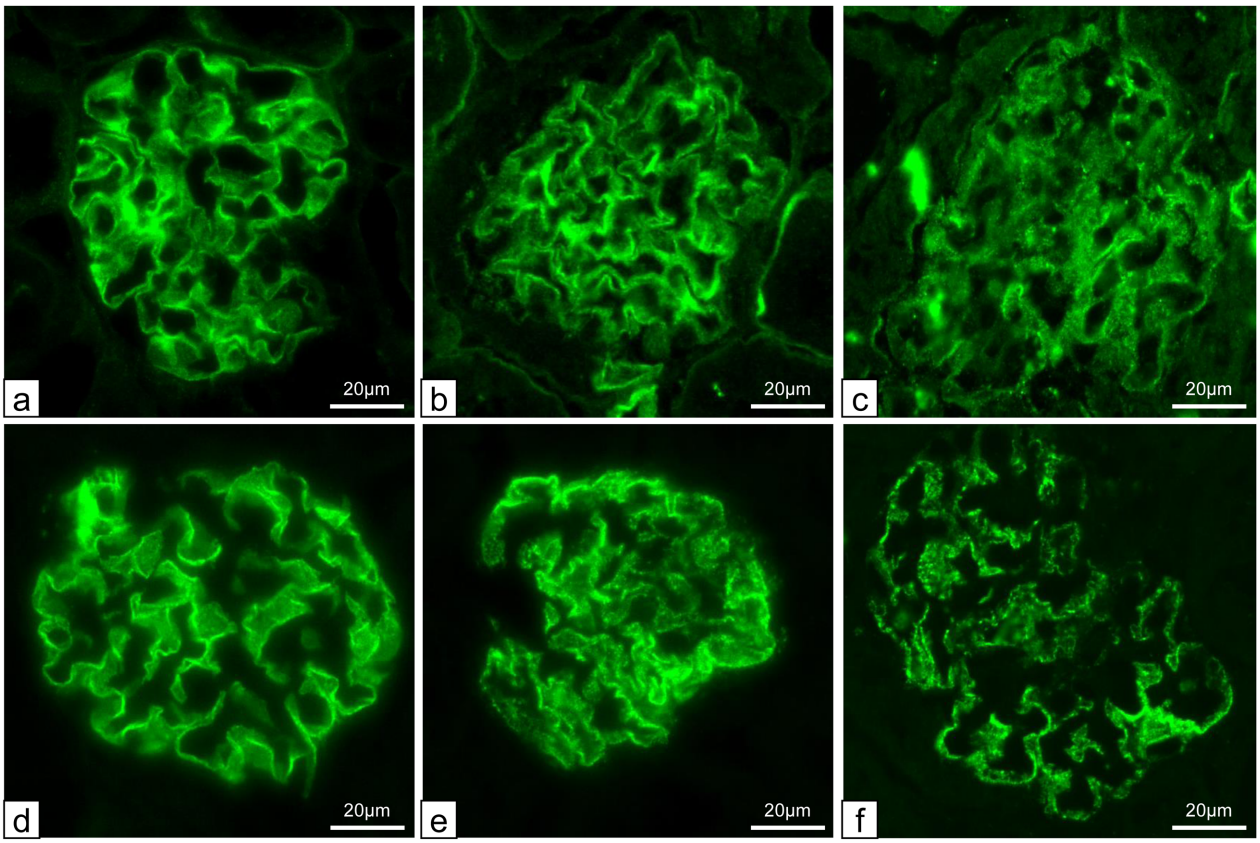

Fig. 5. Expression of nephrin and podocin by immunofluorescence. (a)–(c): anti-nephrin stain. Control mice showed linear pattern along the capillary walls. On the other hand, the staining pattern of both proteins became granular and weak in mito-miceΔ with more than 90% ΔmtDNA accumulation. (d)–(f): anti-podocin stain. Control mice showed linear pattern along the capillary walls. On the other hand, the staining pattern of both proteins became granular and weak in mito-miceΔ with more than 90% ΔmtDNA accumulation. (a,d) C57/B6 control. (b, e) Sample No. 6 (ΔmtDNA 79.3%). (c, f) Sample No. 17 (ΔmtDNA 92.9%).

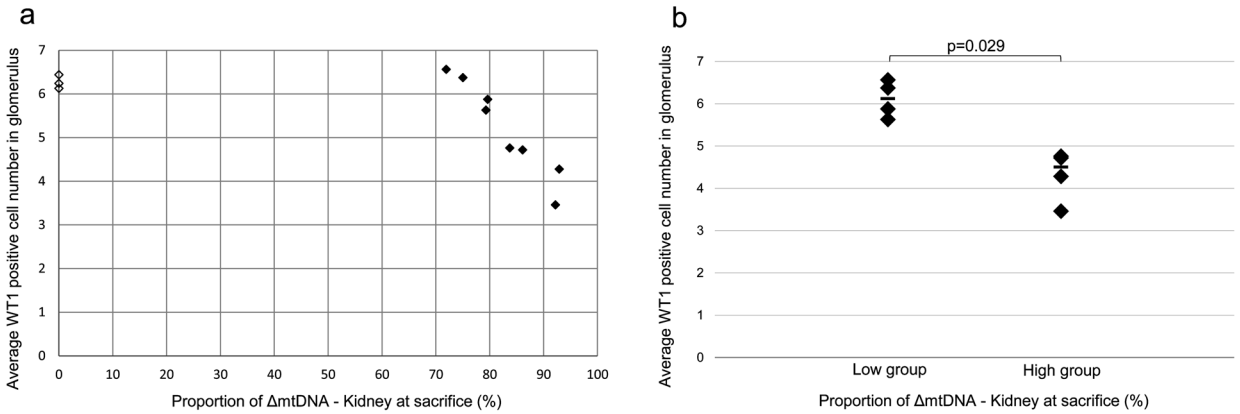

Fig. 6. The relationship between accumulation of ΔmtDNA in the kidney and podocyte number. (a) Overall scatter plot. In control mice (n=3), the median number of WT1 positive cells per glomerulus was 6.2 cells. The number of WT1 positive cells was decreasing in mito-miceΔ with the proportion of ΔmtDNA exceeding a median of 81.7%. (b) Comparing medians of two groups, high proportion of ΔmtDNA group and low proportion group. The WT1-positive podocyte number was statistically significant decreasing in the group with higher proportion of ΔmtDNA in kidney (median 6.1 cells vs median 4.5 cells, *P*=0.029). ◇B6 control (n=3), ◆mito-miceΔ (n=8).

typical for glomerular involvements of FSGS. The electron microscopy findings and podocyte protein expression provided certain evidence for podocyte injury. Furthermore, podocyte loss following foot process effacements and detachment from glomerular basement membrane occurred relatively early stage of glomerular injury and corresponded to the development of proteinuria in mito-miceΔ with ΔmtDNA ratio exceeding 80%.

The affected glomeruli progressed to glomerular sclerotic changes when ΔmtDNA ratio exceeded 90%, suggesting that the podocyte loss is a trigger for developing severe renal failure [17, 19]. The podocyte may thus be a direct target of mitochondrial dysfunction in mitochondrial diseases.

Next, we expanded our analyses to tubular involvements in mito-miceΔ. In this murine models, massive glomerular proteinuria related with glomerular involvements obviously affected tubular involvements, including proteinaceous casts and microcysts in the part of distal tubules. Immunohistochemistry of AQP1 and THP demonstrated that the dilated tubules may be derived from distal nephrons. The casts in dilated tubules contained THP which is originally secreted by thick ascending limb. Extensive formation of THP-positive casts may reflect massive proteinuria originated from upstream glomerular injury. In human FSGS with nephrotic syndrome, proximal tubules frequently show degenerative and regenerative change, and tubular microcysts (dilated distal tubules filled with proteinaceous casts) are commonly seen [19]. This implies that the glomerular injury was early event in renal involvement in mito-miceΔ and resultant proteinuria, at least in part, caused tubular abnormalities. If massive proteinuria persists, interstitial fibrosis appears and spreads widely, finally progressing to renal failure.

The molecular pathology of mito-miceΔ may be different from that of human mitochondrial disease. Mitochondrial myopathy, encephalopathy, lactic acidosis, stroke-like episodes (MELAS) is a classical human mitochondrial disease caused by pathogenic point mutations in mtDNA. In human mitochondrial disease with deletion mutation in mtDNA, only a few cases were reported to be complicated by FSGS [7]. Although careful discussion is needed, our findings may contribute to an understanding of pathogenesis in mitochondrial disease.

In summary, the results suggested the role of podocyte in the evolution of renal involvement in mito-miceΔ. In mito-miceΔ, podocytes were the direct target of mitochondrial dysfunction. Further study on how mitochondrial dysfunction harms podocyte will provide a new insight for mitochondrial disease.

Author Contributions

All authors conceived the study concept and study design. SK, JU, MH, TS and KY wrote the manuscript. SK, JU, MH, TS, RI, MT-K, MK carried out the experiments and analyzed the data. KN, JH and KY supervised the research project. All authors participated in interpretation of the results and writing of the report, and approved the final version.

Conflict of Interests

The authors declare that there are no competing financial interests.

Acknowledgments

We are deeply grateful to Ms. Rie Kikkou, Ms. Mami Kobayashi (University of Tsukuba, Tsukuba, Japan) for their technical support. This work was supported by JSPS KAKENHI Grant Numbers JP19790574 (MH), JP17K09684 (JU), JP19KK0216 (JU), JP21K08220 (KY).

References

1. Wallace DC. Mitochondrial diseases in man and mouse. Science. 1999; 283: 1482–1488. [Medline] [CrossRef]
2. Ng YS, Turnbull DM. Mitochondrial disease: genetics and management. J Neurol. 2016; 263: 179–191. [Medline] [CrossRef]
3. Gorman GS, Chinnery PF, DiMauro S, Hirano M, Koga Y, McFarland R, et al. Mitochondrial diseases. Nat Rev Dis Primers. 2016; 2: 16080. [Medline] [CrossRef]
4. Emma F, Bertini E, Salviati L, Montini G. Renal involvement in mitochondrial cytopathies. Pediatr Nephrol. 2012; 27: 539–550. [Medline] [CrossRef]
5. Hirano M, Konishi K, Arata N, Iyori M, Saruta T, Kuramochi S, et al. Renal complications in a patient with A-to-G mutation of mitochondrial DNA at the 3243 position of leucine tRNA. Intern Med. 2002; 41: 113–118. [Medline] [CrossRef]
6. Hotta O, Inoue CN, Miyabayashi S, Furuta T, Takeuchi A, Taguma Y. Clinical and pathologic features of focal segmental glomerulosclerosis with mitochondrial tRNALeu(UUR) gene mutation. Kidney Int. 2001; 59: 1236–1243. [Medline] [CrossRef]
7. Güçer S, Talim B, Aşan E, Korkusuz P, Ozen S, Unal S, et al. Focal segmental glomerulosclerosis associated with mitochondrial cytopathy: report of two cases with special emphasis on podocytes. Pediatr Dev Pathol. 2005; 8: 710–717. [Medline] [CrossRef]
8. Inoue K, Nakada K, Ogura A, Isobe K, Goto Y, Nonaka I, et al. Generation of mice with mitochondrial dysfunction by introducing mouse mtDNA carrying a deletion into zygotes. Nat Genet. 2000; 26: 176–181. [Medline] [CrossRef]
9. Nakada K, Inoue K, Ono T, Isobe K, Ogura A, Goto YI, et al. Inter-mitochondrial complementation: Mitochondria-specific system preventing mice from expression of disease phenotypes by mutant mtDNA. Nat Med. 2001; 7: 934–940. [Medline] [CrossRef]
10. Nakada K, Sato A, Sone H, Kasahara A, Ikeda K, Kagawa Y, et al. Accumulation of pathogenic DeltamtDNA induced deafness but not diabetic phenotypes in mito-mice. Biochem Biophys Res Commun. 2004; 323: 175–184. [Medline] [CrossRef]
11. Nakada K, Sato A, Yoshida K, Morita T, Tanaka H, Inoue S, et al. Mitochondria-related male infertility. Proc Natl Acad Sci USA. 2006; 103: 15148–15153. [Medline] [CrossRef]
12. Inoue S, Yokota M, Nakada K, Miyoshi H, Hayashi J. Pathogenic mitochondrial DNA-induced respiration defects in he-

matopoietic cells result in anemia by suppressing erythroid differentiation. FEBS Lett. 2007; 581: 1910–1916. [Medline] [CrossRef]
13. Ogasawara E, Nakada K, Hayashi J. Lactic acidemia in the pathogenesis of mice carrying mitochondrial DNA with a deletion. Hum Mol Genet. 2010; 19: 3179–3189. [Medline] [CrossRef]
14. Rossignol R, Faustin B, Rocher C, Malgat M, Mazat JP, Letellier T. Mitochondrial threshold effects. Biochem J. 2003; 370: 751–762. [Medline] [CrossRef]
15. Kriz W. The pathogenesis of 'classic' focal segmental glomerulosclerosis-lessons from rat models. Nephrol Dial Transplant. 2003; 18:(Suppl 6): vi39–vi44. [Medline] [CrossRef]
16. De Vriese AS, Sethi S, Nath KA, Glassock RJ, Fervenza FC. Differentiating Primary, Genetic, and Secondary FSGS in Adults: A Clinicopathologic Approach. J Am Soc Nephrol. 2018; 29: 759–774. [Medline] [CrossRef]
17. Kopp JB, Anders HJ, Susztak K, Podestà MA, Remuzzi G, Hildebrandt F, et al. Podocytopathies. Nat Rev Dis Primers. 2020; 6: 68. [Medline] [CrossRef]
18. Nakada K, Inoue K, Chen CS, Nonaka I, Goto Y, Ogura A, et al. Correlation of functional and ultrastructural abnormalities of mitochondria in mouse heart carrying a pathogenic mutant mtDNA with a 4696-bp deletion. Biochem Biophys Res Commun. 2001; 288: 901–907. [Medline] [CrossRef]
19. D'Agati VD, Stokes MB. Focal segmental glomerulosclerosis. In: Jennette JC, Olson JL, Silva FG, D'Agati VD, editors. Heptinstall's Pathology of the Kidney. 7 ed. Philadelphia: Wolters Kluwer; 2015. pp. 207–254.